Biosensors and Bioelectronics 178 (2021) 113019

Contents lists available at ScienceDirect

Biosensors and Bioelectronics

journal homepage: http://www.elsevier.com/locate/bios

Exploring the trans-cleavage activity of CRISPR-Cas12a for the development of a Mxene based electrochemiluminescence biosensor for the detection of Siglec-5

Kai Zhang [a,*], Zhenqiang Fan [a], Bo Yao [a], Yuedi Ding [a], Jing Zhao [b], Minhao Xie [a], Jianbin Pan [c,**]

[a] NHC Key Laboratory of Nuclear Medicine, Jiangsu Key Laboratory of Molecular Nuclear Medicine, Jiangsu Institute of Nuclear Medicine, Wuxi, Jiangsu, 214063, China

[b] Center for Molecular Recognition and Biosensing, School of Life Sciences, Shanghai University, Shanghai, 200444, PR China

[c] State Key Laboratory of Analytical Chemistry for Life Science and Collaborative Innovation Center of Chemistry for Life Sciences, School of Chemistry and Chemical Engineering, Nanjing University, Nanjing, 210023, China

ARTICLE INFO

Keywords:
CRISPR-Cas12a
Siglec-5
Electrochemiluminescence
Mxene

ABSTRACT

Sialic acid-binding immunoglobulin (Ig)-like lectins (Siglecs) is a type I transmembrane receptor on the cell surface. Siglec-5, as one of the Siglecs family, play an important role as an inhibitory receptor for leukocytes in the human body. The development of novel siglec-5 assays can help to study the pathogenesis of related diseases as well as to develop novel therapeutic drugs. We use catalytic hairpin assembly (CHA) amplification strategy combined with CRISPR-Cas12a's side-cutting feature to build a 2D ultra-thin $Ti_3C_2T_x$ (MXene) based electrochemiluminescence (ECL) biosensor for the detection of Siglec-5. By using this ECL biosensor, the cleavage of CRISPR-Cas12a is reasonably combined with CHA-mediated isothermal amplification, thereby realizing the sensitive amplification assay Siglec-5 with 20.22 fM sensitivity. By introducing pairs of sites that are not in the same double-stranded DNA into the DNA duplex, the hybridization sequence of CRISPR-Cas12a complements the targeting mechanism to enhance indirect Siglec-5 amplification assay. Also, the double-strand DNA (dsDNA) design based on CRISPR-Cas12a amplification allows the same CRISPR RNA (crRNA, also known as guide RNA (gRNA)) to detect the output of DNA duplexes from different intermediate DNAs, which provides a common way for biomarker detection based on the conversion of protein analytes to intermediate DNA strategy. This work extends the application scope of CRISPR-Cas12a to the construction of ECL biosensors, evaluates the role of lectins, which can be used for the biochemical research and clinical diagnosis of protein markers. This is the first investigative work exploring the Trans-Cleavage activity of CRISPR-Cas12a for Mxene-based ECL biosensor establishment to the best of our knowledge.

1. Introduction

Sialic acid-binding immunoglobulin (Ig)-like lectins (Siglecs) is a type I transmembrane receptor on the cell surface, divided into extracellular segment, transmembrane region and intracellular segment. The extracellular segment contains 2 to 17 immunoglobulin-like structural domains and regulates intrinsic and adaptive immunity.(Schauer et al., 1988). It can regulate the immune balance of sepsis, autoimmune diseases, and tumors by recognizing the glycan structure (Macauley et al., 2014). According to the sequence variability, the Siglec family can be divided into two categories: conservative Siglecs, including sialoadhesin, CD22, Siglec-4 and Siglec-15; the other type is CD33-related Siglecs (Walker and Smith 2010). The most common Siglecs on human cells are Siglec-5 and Siglec-9, each of which consists of two intracellular tyrosine signaling units. Siglec-5 can play an important role as an inhibitory receptor for leukocytes in the human body. Siglec-5 has been considered as a potential marker for normal myelopoiesis and acute myelogenous leukemia (AML)(Virgo et al., 2003). Therefore, the development of novel siglec-5 assays can help to study the pathogenesis of related diseases as well as to develop novel therapeutic drugs.

In recent years, the development of isothermal amplification

* Corresponding author.
** Corresponding author.
E-mail addresses: zhangkai@jsinm.org (K. Zhang), jbpan@nju.edu.cn (J. Pan).

https://doi.org/10.1016/j.bios.2021.113019
Received 3 December 2020; Received in revised form 14 January 2021; Accepted 18 January 2021
Available online 26 January 2021

technology and the discovery of CRISPR-Cas family Cas12a flanking splicing features provide a feasible way for double-stranded DNA (ssDNA) amplification (Nouri et al., 2020; Schuster et al., 2020; Smith et al., 2020). The former is a technology that can amplify nucleic acid at a constant temperature. The general term includes recombinase polymerase amplification (RPA), rolling circle amplification (RCA), loop-mediated isothermal amplification (LAMP), transcription-mediated amplification (TMA) et al. RPA is an isothermal amplification technology that can complete exponential nucleic acid amplification in a short time with the participation of recombinase, polymerase, and single-stranded binding protein (Shen et al., 2011). Similar to PCR amplification, RPA can amplify between a given primer pair. The most suitable amplification temperature is 39 °C, and the sensitivity of amplification is also high. This makes it possible to eliminate the dependence of amplification on the PCR, but RPA also has the possibility of non-specific amplification like PCR.

The CRISPR-Cas system is the "adaptive immune system" formed during the long-term evolution of prokaryotes (Sun et al., 2020). The CRISPR-Cas protein is a kind of nuclease, and CRISPR RNA (crRNA, also known as guide RNA (gRNA)) is a short RNA sequence that can interact with the target nucleic acid (Smith et al., 2020). Complementary pairing, distinguishing between dissidents through the protospacer adjacent motif (PAM) site on the target sequence nucleic acid, and guiding the effector CRISPR-Cas protein to shear and degrade the target sequences (Nouri et al., 2020). CRISPR-Cas12a is the second family member of the CRISPR-Cas system, and its effector is the Cas12a-gRNA dimer complex. The gRNA of CRISPR-Cas12a recognizes the T-rich PAM site at the 5′-end of the target sequence with the nucleotide sequence of 5′-TTTV-3' (Kleinstiver et al., 2020). CRISPR-Cas12a/gRNA can specifically shear double-stranded DNA under the targeting effect of gRNA, cis-cutting; when a specific target sequence activates CRISPR-Cas12a, it can perform non-specific shearing single-stranded DNA, that is, reverse style cut or side cut (Gao et al., 2020). When single-stranded DNA is a substrate with a reporter system, the function of the CRISPR-Cas12a side shearing effect biosensor becomes a key molecule for a revolutionary breakthrough in gene detection.

The development of a universal, accurate, and sensitive detection method for disease markers can help in the immediate diagnosis of pathogens, disease types, and disease levels and is of great significance in clinical diagnosis. DNA has been widely used as a bridge in the design of protein detection strategies (Fan et al., 2019). In brief, proteins act on functionalized nucleic acids and displace free DNA, and the displaced DNA can trigger amplification strategies such as isothermal amplification, DNA machine, and entropy-driven amplification to achieve highly sensitive detection of DNA, thus realizing the purpose of protein detection (Zhang et al. 2018, 2019b). In typical DNA isothermal amplification reactions, ssDNA is used as an input to initiate a strand displacement reaction, thereby producing a detectable output. Since discovering the incidental cleavage activity of type II V and VI CRISPR-Cas proteins (which can hydrolyze ssDNA or RNA without distinction), the CRISPR-Cas system has attracted widespread attention in the field biomarkers (RNA, and small molecules) detection, including CRISPR-Cas13a, CRISPR-Cas12a, and CRISPR-Cas12b and CRISPR-Cas14 (Yin et al., 2020). This incidental cleavage activity can efficiently cleave and synthesize fluorescent nucleic acid reporter molecules with several thousand amplification times per second, making these CRISPR-Cas proteins useful in self-signal amplification (Peng et al., 2020). But the work of CRISPR-Cas in protein detection is still rare. Therefore, there is still a great need for a universal and powerful CRISPR-Cas method capable of protein detection in biomedical research and clinical diagnosis.

In the process of seeking signal molecular frameworks used in the construction of various biosensors, two-dimensional (2D) ultra-thin nanosheets have attracted researcher's attention due to their unique framework structure and good modifiable properties (Fang et al., 2018; Peng et al., 2019). In recent years, researchers have developed various 2D nanosheet-based biosensors with good sensitivity and selectivity to detect nucleic acids and proteins (Cai et al., 2019; Ouyang et al., 2020). For example, graphene oxide, C_3N_4, MoS_2, TiS_2, TaS_2 Ta_2NiS_5, and other two-dimensional ultra-thin nanosheets have been successfully applied to the construction of biosensors based on functionalized nucleic acids (Ouyang et al., 2020; Spitz Steinberg et al., 2017). However, some 2D materials (such as MoS_2 and graphene) still have apparent shortcomings, including the following: (i) because the interface of the two-dimensional material is stable, it is difficult to functionalized; (ii) it is easy to stack. These disadvantages result in the loss of some exposed active sites (Jia et al., 2020; Liu et al., 2019; Wen et al., 2018; Zhu et al., 2017). In recent years, 2D ultra-thin $Ti_3C_2T_x$ (MXene), as a new type of 2D material, has attracted attention due to its unique layered structure, easy functionalization and excellent metal conductivity (Huang et al., 2020). The molecular formula of MXenes is $M_n+1X_nT_x$, where M is a transition metal, X is C or N, and T_x represents the degree of surface functionalization. Nowadays, the commonly reported members of MXene include Ti_3C_2, Ti_2C, Nb_2C, V_2C, Ti_3CN, Mo_2C and Ta_4C_3. Such 2D layered materials have the metal conductivity of transition metal carbides and have the super hydrophilic properties of hydroxyl or oxygen-terminated surfaces. These excellent properties make them the materials of choice from energy storage to biosensor construction (Zhang et al., 2019a). Besides, because MXenes can be easily functionalized to modify signal molecules or nanoparticles, MXenes can be used more widely in biosensors' construction (Zeng et al., 2021; Zhang et al., 2020). Based on this, we designed an Electrochemiluminescence (ECL) biosensor based on MXenes for the detection of 2019-nCoV-related proteins. Compared with the traditional chemiluminescence assay, ECL assay has the advantages of controlled reaction, unstable substances can be directly generated in situ on the electrode surface, good reproducibility, high sensitivity, wide dynamic response range, simple instrumentation, low background signal, and long luminescence signal time. Therefore, more and more ECL-based biosensors with high sensitivity and selectivity are designed by researchers and widely used in clinical assays.

We take Siglec-5 as detection target and use catalytic hairpin assembly (CHA) combined with CRISPR-Cas12a′s side-cutting feature to amplify viral target sequence fragments through CHA. A highly sensitive and specific Siglec-5 detection method is reported in this work. The CRISPR-CHA-based Siglec-5 detection method has two essential novelties: By introducing pairs of sites that are not in the same double-stranded DNA into the DNA duplex, the hybridization sequence of CRISPR-Cas12a complements the targeting mechanism to enhance indirect Siglec-5 amplification assay. Also, the double-strand DNA (dsDNA) design based on CRISPR-Cas12a amplification allows the same gRNA to detect the output of DNA duplexes from different intermediate DNAs, which provides a common way for biomarker detection based on the conversion of protein analytes to intermediate DNA strategy. As the gold standard for protein analysis, West-blot requires multiple antibodies, trivial experimental operation steps, and a relatively long time. In contrast, CRISPR-CHA can achieve isothermal detection of a target with only one enzyme (CRISPR-Cas12a). Therefore, we concluded that the system we designed could also provide new ideas for detecting Siglec-5 and providing useful clinical diagnosis tools.

2. Experimental section

2.1. Materials and reagent

All the Oligonucleotides were synthesized from Genscript Biotechnology Co. Ltd. (Nanjing, China), and the sequences are depicted in Table S1. Tris (4,4′-dicarboxylicacid-2,2′-bipyridyl) ruthenium(II) dichloride ($Ru(dcbpy)_3^{2+}$) was purchased from Suna Tech Inc. (Suzhou, China). CRISPR-Cas12a was purchased from NEB (New England BioLabs, Shanghai, China). Chloroauric acid ($HAuCl_4$), 1-ethyl-3-(3-dimethyllaminopropyl)-carbodiimide hydrochloride (EDC), N-

hydroxysuccinimide (NHS) Ethylene imine polymer (PEI), and Nafion117 solution (5%) were purchased from Aladdin Biochemical Technology Co. Ltd. (Shanghai, China). MXene, (Ti_3C_2, 5 mg mL^{-1}) was obtained from Nanjing Xianfeng Nano Co. Ltd. (Nanjing, China). Tris(2-carboxyethyl) phosphine hydrochloride (TCEP) and 6-mercaptohexanol (MCH) were obtained from Sigma-Aldrich (St Louis, MO, USA). Silver nitrate ($AgNO_3$) and sodium borohydride ($NaBH_4$) were purchased from Sinopharm Chemical Reagent Co. Ltd. (Shanghai, China).

2.2. Preparation of $Ru(dcbpy)_3^{2+}$/AuNPs@Ti_3C_2 nanocomposites

According to previous literature reports, we have successfully synthesized PEI@Ru $(dcbpy)_3^{2+}$-Ti_3C_2@AuNPs nanocomposites using the $NaBH_4$ reduction method. First, dissolve 10 mg $Ru(dcbpy)_3^{2+}$ in 4 mL of PBS buffer solution (0.1 M, pH = 7.4). Then, 400 mM EDC and 100 mM NHS were added to the above solution and stirred at room temperature for 2 h. Mix 1 mL of Ti_3C_2 solution (5 mg mL^{-1}) with 5 mL of PEI solution (1% w/v) and add to the above $Ru(dcbpy)_3^{2+}$ solution. Continue to stir the reaction for another 2 h, $Ru(dcbpy)_3^{2+}$ and PEI can be firmly bonded together through the amine bond. Next, add 400 μL $HAuCl_4$ (1%) and 1 mL $NaBH_4$ (0.2 M) to the above solution and stir continuously for 1 h. During this period, $HAuCl_4$ is reduced by $NaBH_4$ to gold nanoparticles (AuNPs) and adheres to Ti_3C_2 to form $Ru(dcbpy)_3^{2+}$/AuNPs@Ti_3C_2 nanocomposite materials. Finally, the nanocomposite was dispersed by centrifugation (12000 rpm), washed with ultrapure water and ethanol several times, and then stored in a PBS (0.1 M, pH = 7.4) buffer solution.

2.3. Non-denaturing polyacrylamide gel electrophoresis (PAGE)

Before electrophoresis analysis, the gel was run at 80 V for 30 min. Then, 10 μL of the sample is evenly mixed with the loading buffer and injected into the sample well of a 20% non-denaturing polyacrylamide (PAGE) gel. Run the electrophoresis on the PAGE gel at 80 V for 2 h. After immersing the gel in the chromogenic solution (Gel-Red) for 30 min, capture the picture on ChemiDoc MP Imager (Bio-Rad, USA).

2.4. ECL biosensor preparation and target assay

Before glassy carbon electrode (GCE) modification, The GCE was carefully polished and cleaned according to the previous method. Then, the GCE surface was covered by 0.5% Nafion. Subsequently, 10 μL Ru $(dcbpy)_3^{2+}$/AuNPs@Ti_3C_2 nanocomposites solution dispersed onto the Nafion/GCE surface and dried at room temperature. After washing several times, the unstable $Ru(dcbpy)_3^{2+}$/AuNPs@Ti_3C_2 nanocomposites were washed off. After washing several times with PBS buffer solution, the modified electrode was immersed in 200 μL of DNA-AgNCs solution for 40 min to modify DNA-AgNCs on the electrode surface. Prior to this step, DNA-AgNCs were prepared in advance according to the following steps: $AgNO_3$ solution (10 μL, 25 mM) was mixed with 1 mL DNA solution (30 μM, 5.0 mM Mg^{2+} in 0.1 M PBS solution, pH 7.4), in which the molar ratio of Ag^+ to template DNA was around 8:1. The mixture was then intensely shocked for 2 min, followed by adding 15 μL $NaBH_4$ solution (25 mM) just as-prepared at 0 °C condition. Continue to oscillate for 1.5 h violently, and the reaction solution was put into refrigerator (4 °C) for 12 h to for the formation of DNA-AgNC. Then 1 mM MCH (5 μL) was dripped on the electrode surface and incubated at 37 °C for 2 h. After washing off the unbound composites with phosphate solution, the $Ru(dcbpy)_3^{2+}$/AuNPs@Ti_3C_2/GCE biosensor was successfully constructed.

In a tube, different concentrations of Siglec-5 were treated with aptamer/intermediate DNA duplex (1 μM) for 1 h to generate intermediate DNA. Then 200 μL CHA reaction sample contained 1 μM H1, 1 μM H2 and generated intermediate DNA solution to conduct reaction at 37 °C for 1 h to generate H1/H2 duplex. Next, 50 μL of CHA reaction solution was added into the cleavage buffer (20 mM tris HCl, 100 mM KCl, 5 mM $MgCl_2$, 5% glycerol and 1 mM DTT) containing 100 nM CRISPR-Cas12a/gRNA. For ECL assay, the $Ru(dcbpy)_3^{2+}$/AuNPs@Ti_3C_2/GCE biosensor was immersed in the above prepared mixed solution for 1-h incubation. The ECL test uses a three-electrode system with a platinum wire as the counter electrode and Ag/AgCl (saturated KCl) as the reference electrode. The CRISPR-Cas12a/gRNA-treated $Ru(dcbpy)_3^{2+}$/AuNPs@Ti_3C_2/GCE biosensor was used as the working electrode. The ECL signals were measured in PBS (0.1 M, pH = 7.4) buffer solution, and the scanning voltage was -1-1.25 V.

2.5. Apparatus

Various morphologies of nanomaterials were tested using field emission transmission electron microscope (TEM) (JEM-2100 F, JEOL, Japan). Electrochemical impedance spectroscopy (EIS) was tested by using an electrochemical workstation (CHI660E, Shanghai Chenhua Instrument Co., Ltd, Shanghai, China). ECL signals were captured using ECL-6B, which was kindly provided by the State Key Laboratory of Analytical Chemistry for Life Sciences, Nanjing University. A three-electrode system was used in this work with a platinum (Pt) wire electrode was used as the counter electrode, an Ag/AgCl electrode was used as the reference electrode, and 3 mm diameter GCE was used as working electrodes.

3. Results and discussion

3.1. The working principle

The sensor based on CRISPR-Cas12a for the detection of novel coronavirus-related proteins consists of four parts: a trigger system, which contains an aptamer sequence of Siglec-5 (named K19) (Lin et al., 2016)and a piece of Intermediate DNA; a probe system, which includes a gRNA and DNA activator for CRISPR-Cas12a; an amplification system, which consists of a set of isothermal amplification systems based on CHA; and a reporter system, which includes a pre-assembled CRISPR-Cas12a effector with gRNA and modified nucleic acid ECL sensor (Scheme 1). The significant binding of CRISPR-Cas12a to double-stranded DNA mainly depends on recognizing double-stranded DNA by gRNA. In the amplification system, based on the previously reported CHA design principles, we designed a CHA amplification program consisting of two DNA hairpins (H1 and H2). The double-stranded DNA formed after the amplification is used for CRISPR-Cas12a binding. Both H1 and H2 consist of a single stem-loop DNA with a 5′ end protrusion. In H1, the 5′ end contains the Intermediate DNA hybridization sequence, and the loop region contains the 5′-TTTA-3′ PAM of CRISPR-Cas12a and the non-target strand (NTS). Simultaneously, the 5′ overhang of H2 contains a sequence that hybridizes with Intermediate DNA/H1 duplex. After H1/H2 duplex formation, Intermediate DNA is replaced by H2 and enters the next cycle, which can further trigger more H1/H2 duplex.

Furthermore, H1/H2 duplex hybridizes with gRNA and becomes an “activator” that binds and activates CRISPR-Cas12a. In this case, the ssDNA sequence on the electrode surface can be cut to keep the ssDNA away from the electrode surface. Since the AgNC in ssDNA can quench the Ti_3C_2/$Ru(bpy)_3^{2+}$ on the electrode surface, the departure of ssDNA and AgNC can restore the ECL signal (For the TEM characterization data of AgNC, please see Fig. S1). Therefore, using this strategy, we can convert the CRISPR-Cas12a system into a sensor to quantify the concentration of Siglec-5, and it can be used as a universal sensor for detecting various target proteins by changing the target aptamer sequences.

3.2. Mechanism investigation of the ECL system

The $Ru(bpy)_3^{2+}$ luminophore embedded in MXene exhibits an anode emission peak in the voltage sweep range of 0–1.25 V, and the co-reactant is PEI also modified on MXene. The proposed ECL

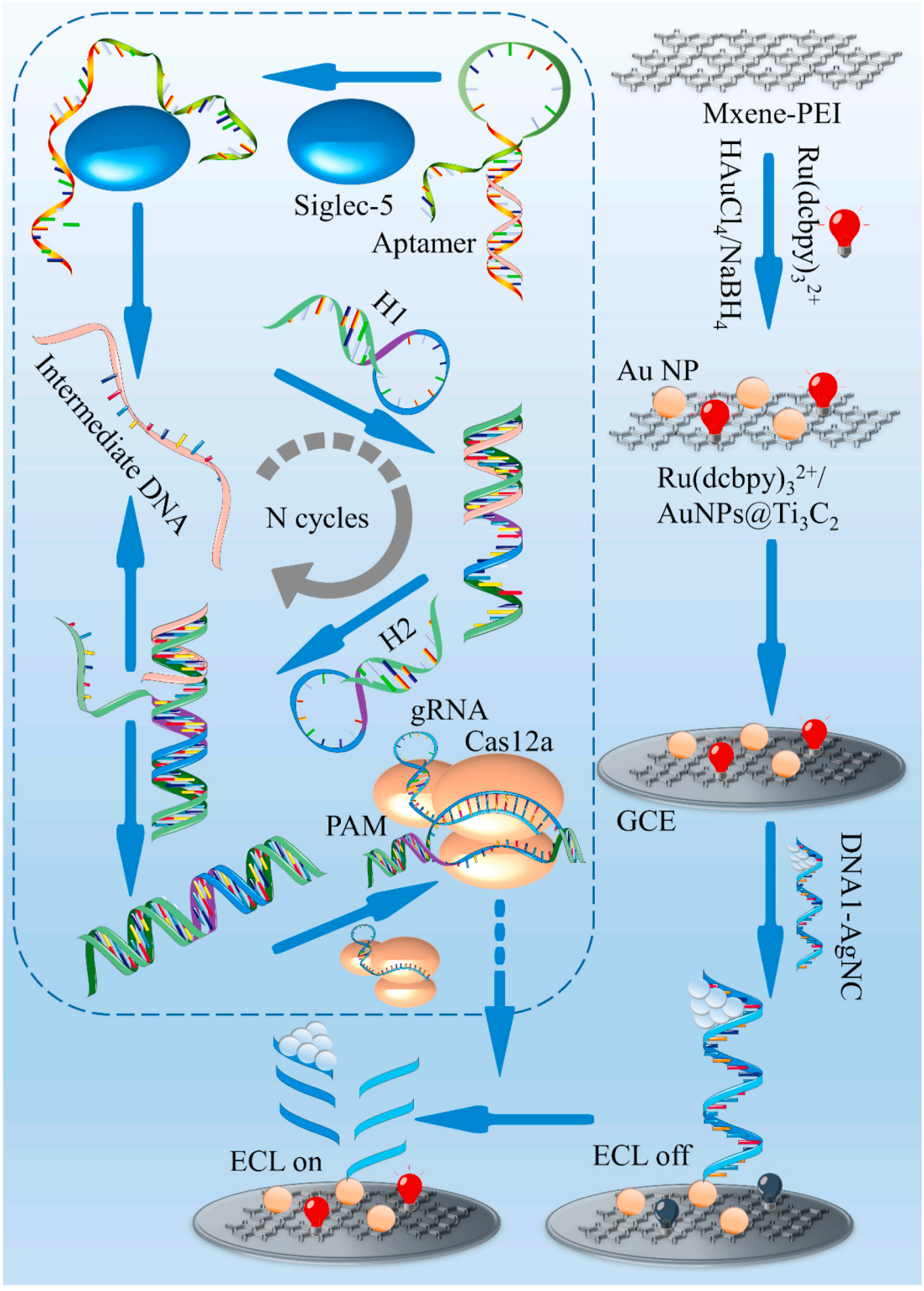

Scheme 1. Construction Process of the Proposed CRISPR-CHA based ECL Biosensor for the Detection of Siglec-5.

luminescence mechanism based on $Ti_3C_2/Ru(bpy)_3^{2+}$–PEI can be expressed by the following formula. PEI is directly oxidized to PEI^+ under an applied voltage, and then directly deprotonated to PEI·radicals (PEI·). PEI·reduce $Ti_3C_2/Ru(bpy)_3^{2+}$ to form $Ti_3C_2/Ru(bpy)_3^{+}$. $Ti_3C_2/Ru(bpy)_3^{+}$ then reacts with $PEI\cdot^+$ in the oxidation state to form $Ti_3C_2/Ru(bpy)_3^{2+}$*. $Ti_3C_2/Ru(bpy)_3^{2+}$* finally transformed into $Ru(bpy)_3^{2+}$ and generate ECL light signal.

$$PEI - e^- \rightarrow PEI^+$$

$$PEI\cdot^+ - H^+ \rightarrow PEI\cdot$$

$$PEI\cdot + Ti_3C_2/Ru(bpy)_3^{2+} \rightarrow Ti_3C_2/Ru(bpy)_3^{+} + product$$

$$PEI\cdot^+ + Ti_3C_2/Ru(bpy)_3^{+} \rightarrow Ti_3C_2/Ru(bpy)_3^{2+*} + product$$

$$Ti_3C_2 / Ru(bpy)_3^{2+*} \rightarrow Ti_3C_2/Ru(bpy)_3^{2+} + h\nu$$

3.3. SEM and TEM characterization of Ti_3C_2 nanosheets, $Ru(dcbpy)_3^{2+}$/AuNPs@Ti_3C_2 nanocomposites and DNA-AgNCs

Fig. S2A shows the TEM image of the prepared single-layer Ti_3C_2, which clearly shows that the single-layer Ti_3C_2 exhibits a smooth sheet structure. Fig. S2B lists the TEM image of $Ru(dcbpy)_3^{2+}$/AuNPs@Ti_3C_2, which shows that AuNP is uniformly attached to the surface of a single layer of Ti_3C_2. After adding $Ru(dcbpy)_3^{2+}$ to the system, the composite $Ru(dcbpy)_3^{2+}$/AuNPs@Ti_3C_2 was successfully synthesized, which can be analyzed and proved by Energy Dispersive Spectrometer (EDS) analysis. As shown in Fig. S2C, the EDS results show that the $Ru(dcbpy)_3^{2+}$/AuNPs@Ti_3C_2 composite contains C, Ti, N, Au and Ru elements. In addition, the main elements of the $Ru(dcbpy)_3^{2+}$/AuNPs@Ti_3C_2 complex were measured by an Energy Dispersive X-ray spectroscopy (EDX) mapping image (Fig. S3). In the Ru 3d region, the binding energies appeared in 2.36 and 2.64 KeV, indicating the successful addition Ru $(dcbpy)_3^{2+}$. The spectra of Au showed at 1.7 KeV and 2.14 KeV, indicating that AuNP was successfully attached to the Ti_3C_2 surface.

3.4. Feasibility of experimental conditions

The CRISPR-Cas12a based amplification strategy was verified by native polyacrylamide gel electrophoresis (PAGE) (Fig. 1A). Because the H1/H2 duplex has a larger molecular weight, it encounters massive steric hindrance during electrophoresis. Therefore, the migration speed of the H1/H2 duplex in lane 6 is slower than that of other single-stranded DNAs. No bright bands are found where the H1/H2 double strands should appear in the intermediate DNA absence (Lane 5). This phenomenon proves that the CHA reaction has not occurred. The electrophoresis picture shows that the formation of H1/H2 duplex requires intermediate DNA triggering.

Then, we studied the ECL signal changes with different conditions in the CRISPR-CHA system. Siglec-5 can cause noticeable ECL signal changes (Fig. 1B curve c, 100 pM target with 100 nM CRISPR-Cas12a). On the contrary, if there is no CRISPR-Cas12a amplification process in the system, the ECL signal does not change significantly (Fig. 1B curve b, 100 pM target without CRISPR-Cas12a). The intensity of the ECL signal triggered by only 100 pM Siglec-5 without CRISPR-Cas12a on the biosensor (Fig. 1B curve b) was almost indistinguishable from that of the biosensor (Fig. 1B curve a). In contrast, the addition of CRISPR-Cas12a to the reaction system dramatically increases the ECL signal intensity (curve c). The above data suggest that CRISPR-Cas12a plays a crucial role in the increase of the signal. Therefore, we can declare that a CRISPR-CHA-based ECL biosensor for Siglec-5 analysis has been successfully developed.

The Electrochemical Impedance Spectroscopy (EIS), as it is an effective method for probing the interfacial properties of electrode surface modifications, has also been used to characterize the interfacial changes during the fabrication of biosensors. The results of EIS measurements performed in 5 mM $K_3[Fe(CN)_6]/K_4[Fe(CN)_6]$ (1:1) to characterize step by step of the GCE were shown in Fig. 1C. The impedance diagram of the bare glassy carbon electrode in Fig. 1C inset) can be seen that the native impedance semicircle diameter is less than 200 (curve a), which indicates that the bare glassy carbon electrode has excellent conductivity and low impedance. When $Ru(dcbpy)_3^{2+}$/AuNPs@Ti_3C_2/GCE modification formed a uniform film on the electrode surface, the impedance of the modified electrode increased significantly (curve b), which was mainly due to the dense $Ru(dcbpy)_3^{2+}$/AuNPs@Ti_3C_2/GCE film hindering the electron transfer, resulting in a larger impedance of

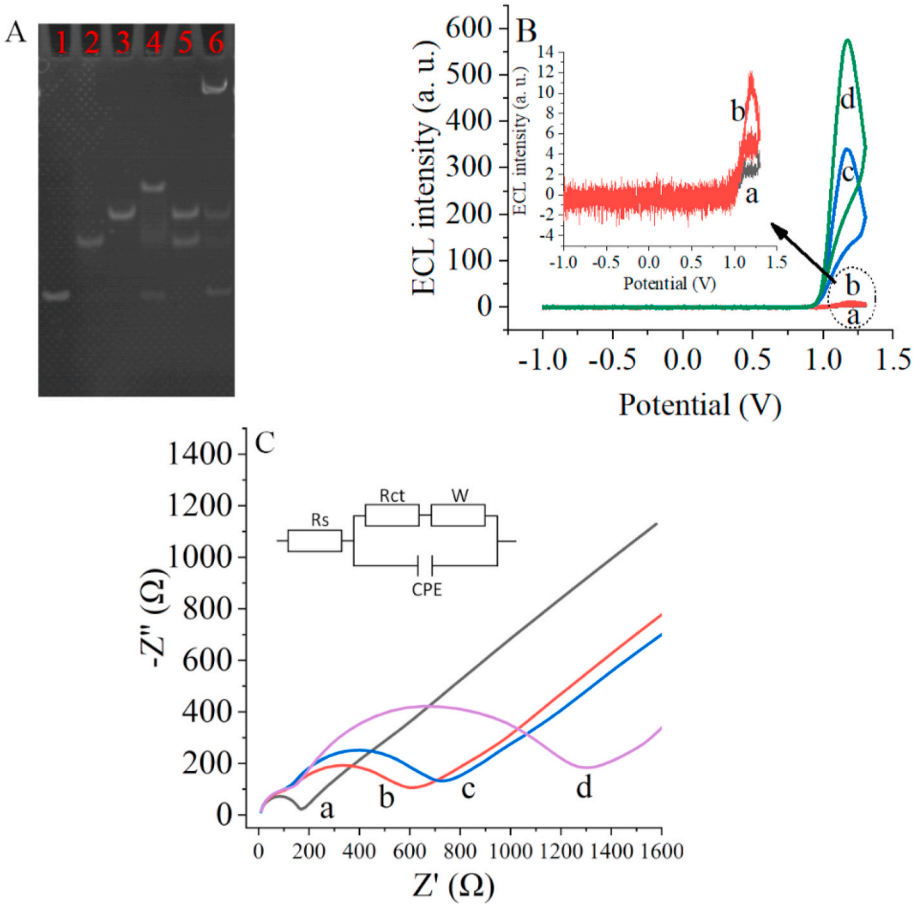

Fig. 1. Feasibility and optimization of the experimental conditions. (A) PAGE image. Lane 1: Intermediate DNA; Lane 2: H1; Lane 3: H2; Lane 4: intermediate DNA; Lane 5: H1+H2; Lane 6, Intermediate DNA + H1+H2. (B) ECL signal changes with different conditions in the CRISPR-CHA system: [a)] Ru $(dcbpy)_3^{2+}$/AuNPs@Ti_3C_2 modified electrode with DNA1-AgNC; b) 100 pM Siglec-5 without CRISPR-Cas12a treated $Ru(dcbpy)_3^{2+}$/AuNPs@Ti_3C_2 modified electrode with DNA1-AgNC; c) 100 pM Siglec-5 with 100 nM treated CRISPR-Cas12a $Ru(dcbpy)_3^{2+}$/AuNPs@Ti_3C_2 modified electrode with DNA1-AgNC; d) $Ru(dcbpy)_3^{2+}$/AuNPs@Ti_3C_2 modified electrode. (C) EIS of the biosensor at different stages of modification: (a) bare GCE; (b) $Ru(dcbpy)_3^{2+}$/AuNPs@Ti_3C modified GCE. (c) DNA1-AgNC and $Ru(dcbpy)_3^{2+}$/AuNPs@Ti_3C modified GCE. (d) MCH, DNA1-AgNC and $Ru(dcbpy)_3^{2+}$/AuNPs@Ti_3C modified GCE. The inset shows the equivalent circuit applied to fit the measurement data, consisting of the ohmic resistance (R_s) of the electrolyte solution, the electronic charge transfer resistance (R_{ct}), a finite length Warburg (W) connected in series, and a constant phase element (CPE) connected in parallel.

the biosensor. When DNA1-AgNC was modified on the gold nanoparticles, the impedance of the sensor increased significantly further (curve c). It indicates that DNA1-AgNC is also hindering electron transport. The subsequent assembly of MCH onto the modified electrode similarly increased the impedance of the biosensor (curve d), as the trapped MCH further hindered electron transfer. Thus, this data indicates the successful assembly of $Ru(dcbpy)_3^{2+}$/AuNPs@Ti_3C_2/GCE biosensor.

3.5. Optimization of the experimental conditions

A suitable pH environment is critical to the sensitivity of the constructed CRISPR-Cas12a-based biosensor. ECL signal strength is tested under weak acid, neutral and weak alkaline conditions. When the ECL intensity is in the range of pH 6.0 to pH 9.0 (Fig. 2A), the signal first increases and then decreases slightly, reaching the maximum ECL intensity value at pH = 7.5. The reason for the maximum signal at pH = 7.5 may be that CRISPR-Cas12a has the highest shear activity at this pH (Yuan et al., 2020; Zhou et al., 2020). Therefore, pH = 7.5 was chosen as the optimal reaction condition. Next, we optimized the concentration of the CRISPR-Cas12a enzyme, and we chose different concentrations of CRISPR-12a to add to the reaction system (Fig. 2B). Other conditions, including nucleic acid concentration and reaction time, were unchanged. It was found that with the change of CRISPR-Cas12a concentration, the ECL signal increased. When the CRISPR-Cas12a concentration reached 100 nM, the ECL signal reached its maximum value. The reason for this phenomenon may be that in the reaction system we designed, the concentration of 100 nM CRISPR-Cas12a reached saturation, and larger concentrations of CRISPR-Cas12a did not increase the shear capacity and therefore did not cause a further increase in ECL signal. Therefore, we choose 100 nM for the next analyte detection experiment.

3.6. Assay performance

Furthermore, we studied the ECL signal response of CRISPR-CHA to different concentrations of Siglec-5. Here, ECL intensity were measured in the presence and absence of Siglec-5, respectively. Fig. 3A and B shows that the ECL intensity increases as the Siglec-5 concentration increases from 20 fM to 100 pM. In addition, Fig. 3C shows the relationship between the concentration of Siglec-5 and the value of the ECL signal. The graph shows that as the concentration of Siglec-5 increases, the ECL signal is subsequently enhanced, and the signal almost reaches a maximum when the concentration of sigle-5 is 10 pM. It is possible that this phenomenon is due to the fact that the DNA1-AgNC on the electrode surface has been completely cleaved. The inset of Fig. 3C inset shows the linear relationship between the Siglec-5 and ECL intensity from 20 to 1000 fM. The linear relationship is in accordance with the equation: Y = 0.236X+8.075 (R^2 = 0.9936). In this equation, X is the concentration of Siglec-5 and Y is the signal value of ECL. The limit of detection (LOD) of the biosensor calculated by 3σ/slope method was 29.36 fM, which is more sensitive than the method proposed by Lin et al. (LOD of 0.27 nM) (Lin et al., 2016). The σ is the standard deviation when measuring blank, and the slope is obtained from the above equation. The excellent detection sensitivity is attributed to the isothermal amplification efficiency of CHA and the shearing efficiency of CRISPR-Cas12a. Therefore, our design provides an ultra-sensitive method for analyzing Siglec-5.

To further study whether the practicability of the proposed Siglec-5 detection strategy can be tolerated in real samples, Siglec-5 in 10-fold diluted human serum was added with different concentrations of Siglec-5 before detection Siglec-5 concentration by using our CRISPR-CHA based biosensor. When Siglec-5 concentrations were added to human serum at different doses, the assay showed a gradual increase in ECL intensity (Fig. 4). Our results indicate that the Siglec-5 analysis platform may potentially be widely used to detect Siglec-5 in complex biological samples.

3.7. Specificity assay

The specificity of the CRISPR-CHA-based electrochemiluminescence biosensor to Siglec-5 was evaluated through two control experiments: (a) the sequence contains gRNA analogous with different mutation sites, and (b) four unrelated proteins (AFP, CEA, BSA, and NF-κB p50 (selected at random), none of them can bind to K19 aptamer. Three DNA sequences (gRNA1, gRNA2, and gRNA3) with mutant bases in gDNA are used (Table S1). Add Siglec-5 at a concentration of 10 pM to different reaction systems, only gRNA is replaced by gRNA1, gRNA2, and gRNA3 in the system, and the other conditions remain unchanged. After two amplification steps, neither the gRNA1, gRNA2, nor the gRNA3 system caused significant ECL signal changes, but the ECL signal of the gRNA system only changed significantly (Fig. 5A). The reason for this difference is the ability of gRNA to recognize double-stranded H1/H2 duplexes. Because gRNA1, gRNA2, and gRNA3 have mutation sites that cannot bind to the H1/H2 duplex, the cleavage activity of CRISPR-Cas12a cannot be activated. The main challenge of detecting protein markers is distinguishing other proteins, which is essential to understand the preclinical diagnosis and pathogenic mechanism of protein markers. Therefore, the specificity of the proposed biosensor was

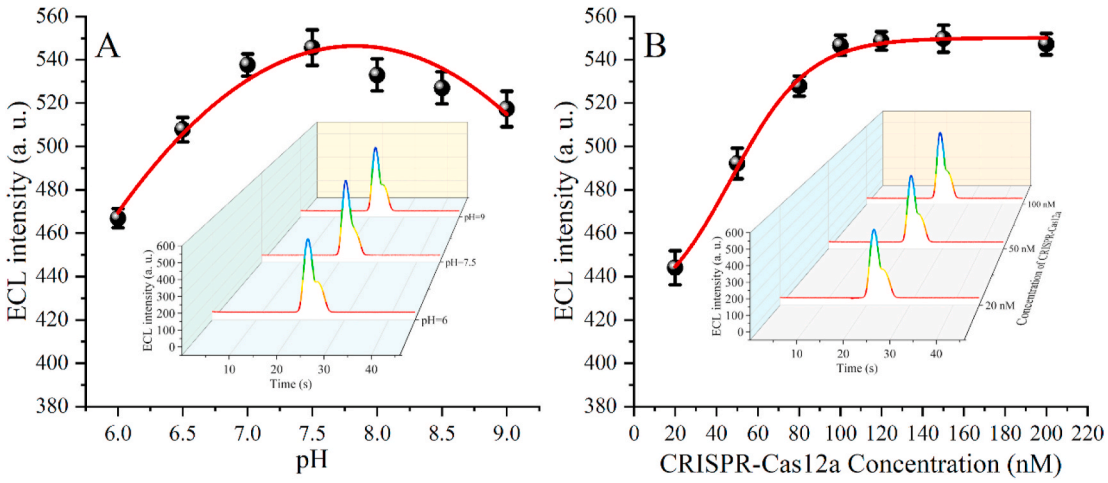

Fig. 2. Optimization of the Experimental Conditions. (A) Plots of ECL signal values versus pH. The inset shows the ECL spectra at different pH values (pH=6, pH=7.5 and pH=9). (B) Plot of ECL signal values versus CRISPR−Cas12a. The inset shows the ECL spectra at different values of CRISPR−Cas12a concentration. Each point and error bar represents the mean value ± standard deviation (mean ± SD) expression of three measurements on the same sample.

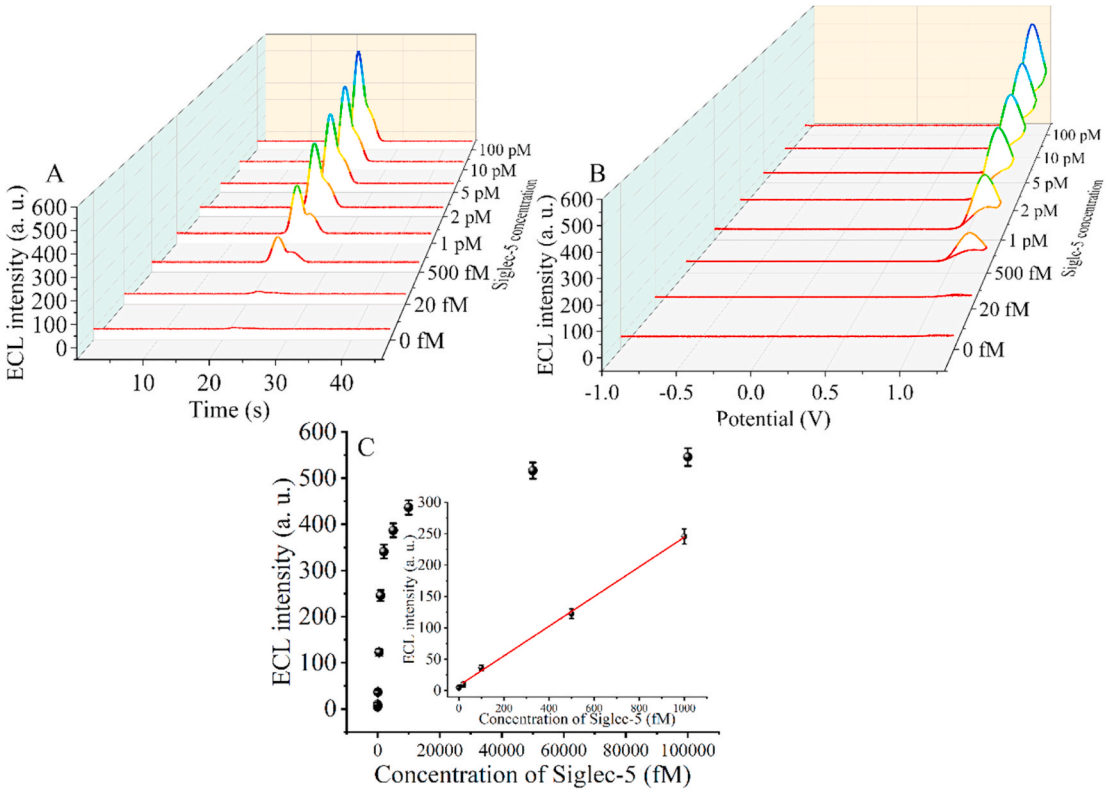

Fig. 3. ECL intensity of the CRISPR-CHA based Ru(dcbpy)$_3^{2+}$/AuNPs@Ti_3C_2 biosensor for detecting Siglec-5. (A) The relationship of the time-based ECL intensity with the concentration of Siglec-5; (B) The relationship of the potential-based ECL intensity with the concentration of Siglec-5; (C) Calibration values for the relationship between the ECL intensity and the Siglec-5 concentration. The inset shows the linear part of the relationship between ECL intensity and Siglec-5 concentrations. Each point and error bar represents the mean value ± standard deviation (mean ± SD) expression of three measurements on the same sample.

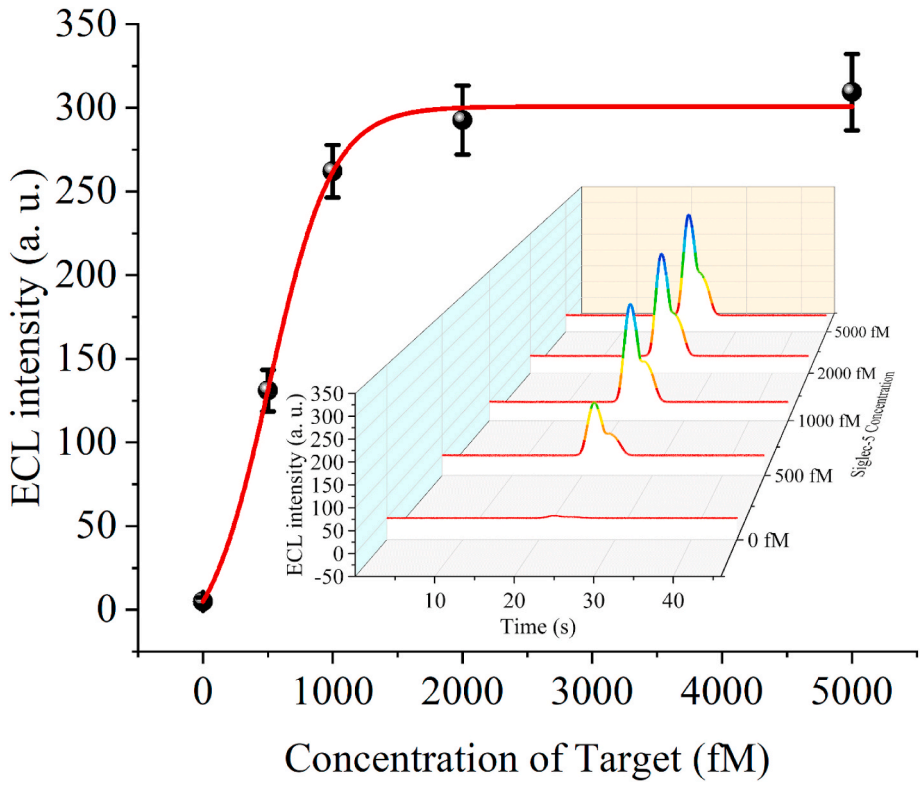

Fig. 4. Detection of Siglec-5 in 10-fold diluted human serum. The relationship between the ECL intensity and the Siglec-5 concentration. Inset shows the relationship of the time-based ECL intensity with the added concentration of Siglec-5. Each point and error bar represents the mean value ± standard deviation (mean ± SD) expression of three measurements on the same sample.

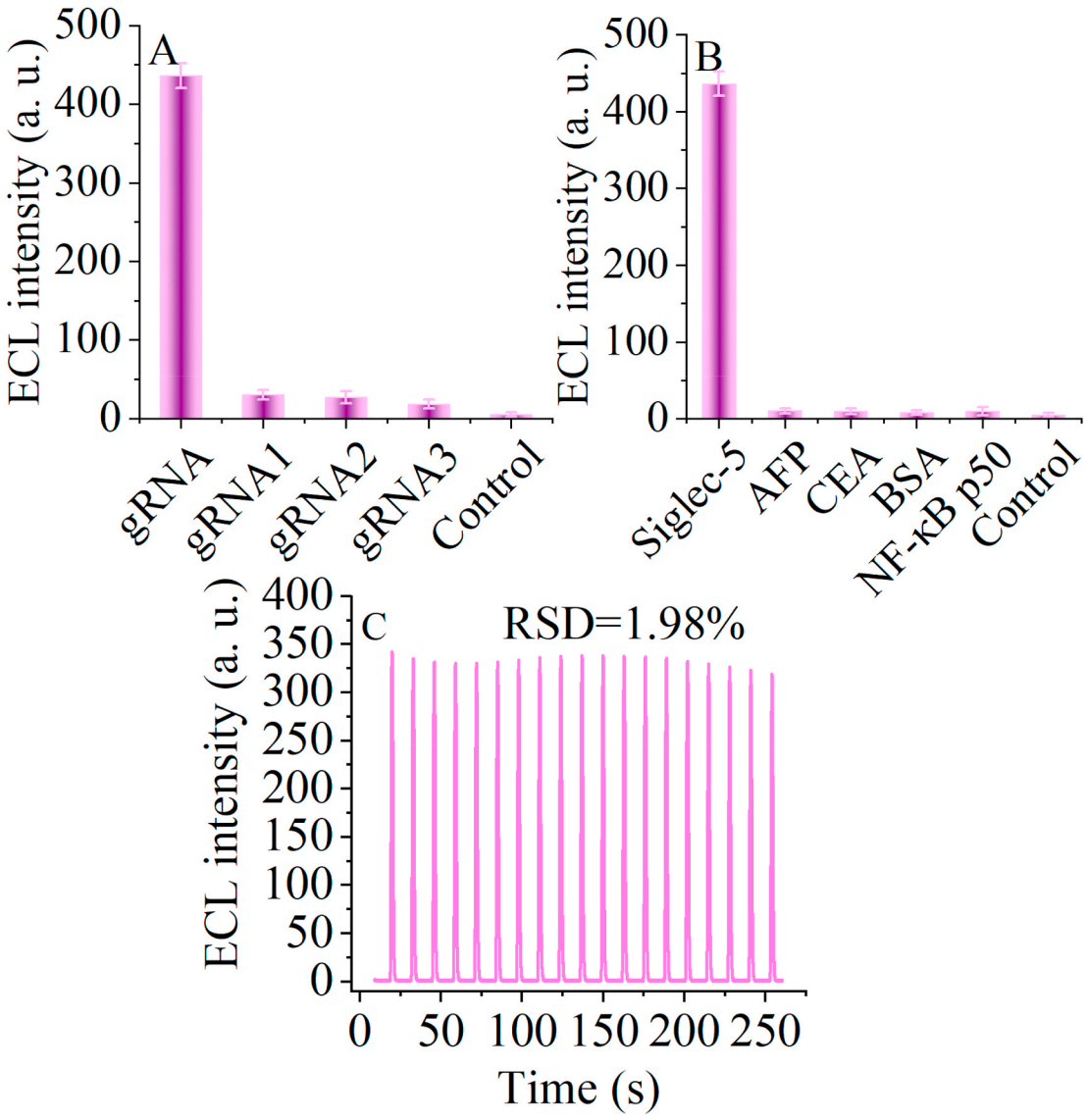

Fig. 5. Specificity assay of the CRISPR-CHA based ECL biosensor and the stability of the biosensor. (A) The sequence contains gRNA analogs with different mutation sites; (b) Target and four unrelated proteins (AFP, CEA, BSA, and NF-κB p50); (C) The stability of the biosensor. Each point and error bar represents the mean value ± standard deviation (mean ± SD) expression of three measurements on the same sample.

studied in the presence of other control proteins. The ECL signal generated by the control protein was only higher than that of the control experiment (without Siglec-5) is slightly larger, which is significantly higher than the ECL signal of Siglec-5 (Fig. 5B). This high selectivity comes from the high recognition ability of the aptamer sequence for Siglec-5. These results show that our CRISPR-CHA-based electrochemiluminescence biosensor has high specificity for Siglec-5 detection.

In addition, we explored the stability of the biosensor by measuring the ECL signal values for 19 cycles after 2 pM Siglec-5 was applied to the biosensor. The calculated relative standard deviation (RSD) is within an acceptable range (5%), indicating that our Ti_3C_2-based ECL biosensor has good reproducibility and stability (Fig. 5C).

4. Conclusions

In conclusion, we have proposed a Mxene based ECL biosensor for detection of Siglec-5 by combining CRISPR-Cas12a amplification with the $Ru(dcbpy)_3^{2+}$/AuNPs@Ti_3C_2 nanocomposite as the emitter. This is the first investigative work exploring the Trans-Cleavage activity of CRISPR-Cas12a for Mxene-based ECL biosensor establishment to the best of our knowledge. In this assay, the cleavage of CRISPR-Cas12a is reasonably combined with CHA-mediated isothermal amplification, thereby realizing the amplification detection of Siglec-5 with 20.22 fM. Considering the CHA isothermal amplification method's modularity and scalability, the strategy can be used for the analysis and detection of different proteins. Since the activation of CRISPR-Cas12a requires double-stranded DNA in the strategy, the property that the product after CHA amplification is double-stranded DNA allows the combination of isothermal amplification and activation of CRISPR-Cas12a. In addition, since the requirement for activation of CRISPR-Cas12a activity is 5′-TTTV-3′ PAM site (four base pairs) in the double-stranded DNA, the CHA-amplified double-stranded product DNA easily meets this requirement. Compared with the detection based on other nicking enzymes, it has unparalleled advantages in versatility and sensitivity. MXene has the metal conductivity of transition metal carbides and have the super hydrophilic properties of hydroxyl or oxygen-terminated surfaces. Therefore, this MXene based biosensor is easy to construct and stable. More importantly, the improved analytical performance was achieved without compromising the simplicity of the biosensor, as the system requires only one-step incubation of the product after the

CRISPR-Cas12a reaction. Therefore, this work extends the application scope of CRISPR-Cas12a to the construction of protein biosensors, evaluates the role of lectins, which can be used for the biochemical research and clinical diagnosis of protein markers.

CRediT authorship contribution statement

Kai Zhang: Conceptualization, Writing - review & editing. **Zhenqiang Fan:** Data curation, Characterization, Software. **Bo Yao:** Data curation, Characterization, Software. **Yuedi Ding:** Data curation, Characterization, Software. **Jing Zhao:** Data curation, Experimental discussion. **Minhao Xie:** Writing - review & editing. **Jianbin Pan:** Writing - review & editing, Conceptualization.

Declaration of competing interest

The authors declare that they have no known competing financial interests or personal relationships that could have appeared to influence the work reported in this paper.

Acknowledgment

This work was supported by the National Natural Science Foundation of China (21705061), Shanghai Pujiang Program (2019PJD018), the Jiangsu Provincial Key Medical Discipline (Laboratory) (ZDXKA2016017), and the Innovation Capacity Development Plan of Jiangsu Province (BM2018023).

Appendix A. Supplementary data

Supplementary data to this article can be found online at https://doi.org/10.1016/j.bios.2021.113019.

References

Cai, D., Lu, M., Li, L., Cao, J., Chen, D., Tu, H., Li, J., Han, W., 2019. Small 15 (44), 1902605.
Fan, Z., Wang, J., Hao, N., Li, Y., Yin, Y., Wang, Z., Ding, Y., Zhao, J., Zhang, K., Huang, W., 2019. Chem. Commun. 55 (79), 11892–11895.
Fang, Y., Yang, X., Chen, T., Xu, G., Liu, M., Liu, J., Xu, Y., 2018. Sensor. Actuator. B Chem. 263, 400–407.
Gao, Z., Fan, M., Das, A.T., Herrera-Carrillo, E., Ben, B., 2020. Nucleic Acids Res. 48 (10), 5527–5539.
Huang, K., Li, C., Li, H., Ren, G., Wang, L., Wang, W., Meng, X., 2020. ACS Applied Nano Materials.
Jia, Y., Yi, X., Li, Z., Zhang, L., Yu, B., Zhang, J., Wang, X., Jia, X., 2020. Talanta 219, 121308.
Kleinstiver, B.P., Sousa, A.A., Walton, R.T., Tak, Y.E., Hsu, J.Y., Clement, K., Welch, M. M., Horng, J.E., Malagon-Lopez, J., Scarfo, I., Maus, M.V., Pinello, L., Aryee, M.J., Joung, J.K., 2020. Nat. Biotechnol. 38 (7), 901, 901.
Lin, S., Lu, L., Kang, T.-S., Mergny, J.-L., Leung, C.-H., Ma, D.-L., 2016. Anal. Chem. 88 (20), 10290–10295.
Liu, Y., Guo, W., Su, B., 2019. Chin. Chem. Lett. 30 (9), 1593–1599.
Macauley, M.S., Crocker, P.R., Paulson, J.C., 2014. Nat. Rev. Immunol. 14 (10), 653–666.
Nouri, R., Jiang, Y., Lian, X.L., Guan, W., 2020. ACS Sens. 5 (5), 1273–1280.
Ouyang, X., Tang, L., Feng, C., Peng, B., Liu, Y., Ren, X., Zhu, X., Tan, J., Hu, X., 2020. Biosens. Bioelectron. 164, 112328.
Peng, S., Tan, Z., Chen, S., Lei, C., Nie, Z., 2020. Chem. Sci. 11 (28), 7362–7368.
Peng, X., Zhang, Y., Lu, D., Guo, Y., Guo, S., 2019. Sensor. Actuator. B Chem. 286, 222–229.
Schauer, R., Fischer, C., Lee, H., Ruch, B., Kelm, S., 1988. Sialic Acids as Regulators of Molecular and Cellular Interactions. Springer Berlin Heidelberg, Berlin, Heidelberg, pp. 5–23.
Schuster, F., Aldag, P., Frenzel, A., Hadeler, K.-G., Lucas-Hahn, A., Niemann, H., Petersen, B., 2020. Sci. Rep. 10 (1).
Shen, F., Davydova, E.K., Du, W., Kreutz, J.E., Piepenburg, O., Ismagilov, R.F., 2011. Anal. Chem. 83 (9), 3533–3540.
Smith, C.W., Nandu, N., Kachwala, M.J., Chen, Y.-S., Uyar, T.B., Yigit, M.V., 2020. Biochemistry 59 (15), 1474–1481.
Spitz Steinberg, R., Cruz, M., Mahfouz, N.G.A., Qiu, Y., Hurt, R.H., 2017. ACS Nano 11 (6), 5670–5679.
Sun, W., Wang, J., Hu, Q., Zhou, X., Khademhosseini, A., Gu, Z., 2020. Sci. Adv. 6 (21).
Virgo, P., Denning-Kendall, P.A., Erickson-Miller, C.L., Singha, S., Evely, R., Hows, J.M., Freeman, S.D., 2003. Br. J. Haematol. 123 (3), 420–430.
Walker, J.A., Smith, K.G.C., 2010. Insect ence 123 (3), 314–325.
Wen, W., Song, Y., Yan, X., Zhu, C., Du, D., Wang, S., Asiri, A.M., Lin, Y., 2018. Mater. Today 21 (2), 164–177.
Yin, K., Ding, X., Li, Z., Zhao, H., Cooper, K., Liu, C., 2020. Anal. Chem. 92 (12), 8561–8568.
Yuan, T., Mukama, O., Li, Z., Chen, W., Zhang, Y., de Dieu Habimana, J., Zhang, Y., Zeng, R., Nie, C., He, Z., Zeng, L., 2020. Analyst 145 (19), 6388–6394.
Zeng, R., Wang, W., Chen, M., Wan, Q., Wang, C., Knopp, D., Tang, D., 2021. Nano Energy 82, 105711.
Zhang, H., Wang, Z., Wang, F., Zhang, Y., Wang, H., Liu, Y., 2020. Anal. Chem. 92 (7), 5546–5553.
Zhang, H., Wang, Z., Zhang, Q., Wang, F., Liu, Y., 2019a. Biosens. Bioelectron. 124–125, 184–190.
Zhang, K., Huang, W., Li, H., Xie, M., Wang, J., 2019b. Biosens. Bioelectron. 132, 310–318.
Zhang, N., Shi, X.-M., Guo, H.-Q., Zhao, X.-Z., Zhao, W.-W., Xu, J.-J., Chen, H.-Y., 2018. Anal. Chem. 90 (20), 11892–11898.
Zhou, R., Li, Y., Dong, T., Tang, Y., Li, F., 2020. Chem. Commun. 56 (24), 3536–3538.
Zhu, C., Du, D., Lin, Y., 2017. Biosens. Bioelectron. 89, 43–55.